

*Supporting Information*

## **An azido-bridged [Fe<sup>II</sup><sub>4</sub>] grid-like molecule showing spin crossover behaviour**

Zhilin Guo,<sup>a, b</sup> Maolin You,<sup>a, c</sup> Yi-Fei Deng,<sup>a</sup> Qiang Liu,<sup>d</sup> Yin-Shan Meng,<sup>d</sup> Zoe Pikramenou,<sup>\*b</sup> and Yuan-Zhu Zhang<sup>\*a</sup>

<sup>a</sup> Department of Chemistry, Southern University of Science and Technology, Shenzhen, 518055, P. R. China.

<sup>b</sup> School of Chemistry, The University of Birmingham, Edgbaston B15 2TT, United Kingdom.

<sup>c</sup> Department of Chemistry, National University of Singapore, Science Drive 3, Singapore 117543

<sup>d</sup> State Key Laboratory of Fine Chemicals, Dalian University of Technology, 2 Linggong Rd, Dalian 116024, P. R. China

Email: z.pikramenou@bham.ac.uk; zhangyz@sustech.edu.cn

**Crystallography.** X-ray data for **1** and **2** were collected on a Bruker D8 VENTURE diffractometer with graphite monochromated Mo K $\alpha$  ( $\lambda = 0.71073 \text{ \AA}$ ) and Cu K $\alpha$  ( $\lambda = 1.54178 \text{ \AA}$ ) radiation, respectively. Lorentz/polarization corrections were applied during data reduction and the structures were solved with the SHELXT solution program using Intrinsic Phasing.<sup>[1]</sup> Refinements were performed by full-matrix least squares minimization (SHELXL) on  $F^2$ .<sup>[2]</sup> Anisotropic thermal parameters were used for the non-hydrogen atoms. Hydrogen atoms were added at calculated positions and refined using a riding model. Weighted R factors (wR) and the goodness-of-fit (S) values are based on  $F^2$ ; conventional R factors (R) are based on F, with F set to zero for negative  $F^2$ . Since the solvent molecules in **1** could not be completely modelled due to the disorder, a part of Q peaks were subtracted by the SQUEEZE program implemented in Olex2. As a result, 272.6 electrons were found in a total solvent accessible volume of  $1035.3 \text{ \AA}^3$  for **1** per unit cell. Combined with the definition in the residual density map, we attribute this to the presence of four CHCl<sub>3</sub> and two CH<sub>3</sub>OH per unit cell which account for 268 electrons that is consistent with the SQUEEZE calculations.

## References

- [1] Sheldrick, G.M. *Acta Cryst.* **2015**, *A71*, 3-8.
- [2] Sheldrick, G.M. *Acta Cryst.* **2015**, *C71*, 3-8.

**Table S1.** Selected Crystallographic data of **1** and **2**.

Compound	<b>1</b>		<b>2</b>		
Empirical formula	C <sub>168</sub> H <sub>173</sub> B <sub>4</sub> Cl <sub>15</sub> Fe <sub>4</sub> N <sub>40</sub> O <sub>3</sub>		C <sub>156</sub> H <sub>126</sub> B <sub>4</sub> Fe <sub>4</sub> N <sub>30</sub>		
Formula weight	3598.85		2687.50		
Radiation	MoK $\alpha$ ( $\lambda$ = 0.71073)		CuK $\alpha$ ( $\lambda$ = 1.54178)		
Crystal size/mm <sup>3</sup>	0.30 $\times$ 0.25 $\times$ 0.15		0.25 $\times$ 0.25 $\times$ 0.20		
Crystal system	Triclinic		Tetragonal		
Space group	P-1		I4 <sub>1</sub> /a		
Temp.	100 K	100 K	150 K	200 K	300 K
CCDC deposit	2015661	2015655	2078512	2015657	2015660
a/Å	18.0455(8)	17.2401(3)	17.2652(8)	17.3036(3)	17.4466(3)
b/Å	19.1164(8)	17.2401(3)	17.2652(8)	17.3036(3)	17.4466(3)
c/Å	28.9018(12)	42.898(1)	43.062(3)	43.1803(10)	43.6969(13)
$\alpha$ /°	89.217(2)	90	90	90	90
$\beta$ /°	72.662(2)	90	90	90	90
$\gamma$ /°	62.820(2)	90	90	90	90
Volume/Å <sup>3</sup>	8377.7(6)	12750.2(5)	12836.1(15)	12928.8(5)	13300.6(6)
Z	2	4	4	4	4
$\rho_{\text{calc}}$ /cm <sup>3</sup>	1.212	1.400	1.391	1.381	1.342
$\mu$ /mm <sup>-1</sup>	0.449	4.124	4.097	4.067	3.954
F(000)	3192.0	5584.0	5584.0	5584.0	5584.0
2 $\theta$ range /°	2.628 to 55.018	8.03 to 136.6	5.51 to 130.3	10.2 to 136.8	7.91 to 130.3
Reflections collected/unique	200308/37755	37412/5831	26305/5831	26305/5831	26215/5667
R <sub>int</sub>	0.0545	0.0565	0.0794	0.0490	0.0622
R <sub>sigma</sub>	0.0473	0.0307	0.0739	0.0325	0.0590
Goodness-of-fit on F <sup>2</sup>	1.030	1.068	0.996	1.057	1.024
Final R indexes [I > 2 $\sigma$ (I)]	R <sub>1</sub> = 0.0493, wR <sub>2</sub> = 0.1181	R <sub>1</sub> = 0.0369, wR <sub>2</sub> = 0.0965	R <sub>1</sub> = 0.0660, wR <sub>2</sub> = 0.1707	R <sub>1</sub> = 0.0335, wR <sub>2</sub> = 0.0904	R <sub>1</sub> = 0.0479, wR <sub>2</sub> = 0.1238
Final R indexes [all data]	R <sub>1</sub> = 0.0759, wR <sub>2</sub> = 0.1322	R <sub>1</sub> = 0.0459, wR <sub>2</sub> = 0.1011	R <sub>1</sub> = 0.1027, wR <sub>2</sub> = 0.1994	R <sub>1</sub> = 0.0466, wR <sub>2</sub> = 0.0958	R <sub>1</sub> = 0.0748, wR <sub>2</sub> = 0.1408
Largest diff. peak/hole / e Å <sup>-3</sup>	0.59/-0.98	0.70/-0.23	0.54/-0.31	0.34/-0.27	0.28/-0.14

**Table S2.** Selected bond distance [ $\text{\AA}$ ] and angles [deg] of **1** at 100 K.

Fe1-N1	2.159(2)	Fe4-N16	2.183(2)	N4-Fe2-N9	175.68(7)
Fe1-N3	2.209(1)	Fe4-N18	2.179(2)	N4-Fe2-N7	109.20(7)
Fe1-N19	2.154(1)	Fe4-N22	2.196(1)	N4-Fe2-N34	93.30(7)
Fe1-N21	2.220(1)	Fe4-N24	2.160(2)	N4-Fe2-N25	84.63(7)
Fe1-N25	2.084(1)	Fe4-N28	2.103(1)	N4-Fe2-N6	72.48(7)
Fe1-N28	2.123(1)	Fe4-N31	2.121(2)	N15-Fe3-N10	172.34(7)
Fe2-N4	2.223(2)	N3-Fe1-N21	175.14(7)	N15-Fe3-N12	108.78(7)
Fe2-N6	2.151(2)	N3-Fe1-N19	111.02(7)	N15-Fe3-N34	93.04(7)
Fe2-N7	2.159(2)	N3-Fe1-N28	91.64(7)	N15-Fe3-N31	85.95(7)
Fe2-N9	2.222(1)	N3-Fe1-N25	86.10(7)	N15-Fe3-N13	72.48(7)
Fe2-N25	2.125(1)	N3-Fe1-N1	72.37(7)	Fe1-N25-Fe2	120.86(9)
Fe2-N34	2.079(2)	N16-Fe4-N22	173.87(7)	Fe1-N28-Fe4	118.79(9)
Fe3-N10	2.212(1)	N16-Fe4-N24	113.55(7)	Fe3-N34-Fe2	120.40(9)
Fe3-N12	2.157(2)	N16-Fe4-N31	86.97(7)	Fe3-N31-Fe4	118.89(9)
Fe3-N13	2.179(2)	N16-Fe4-N28	87.41(7)		
Fe3-N15	2.221(2)	N16-Fe4-N18	72.64(7)		
Fe3-N31	2.120(1)				
Fe3-N34	2.079(2)				

**Table S3.** Selected bond distance [ $\text{\AA}$ ] and angles [deg] of **2** at different temperatures.

	100 K	150 K	200 K	300 K
Fe1-N1	1.976(0)	1.999(4)	1.985(8)	2.150(3)
Fe1-N2	1.920(9)	1.940(4)	1.938(7)	2.141(2)
Fe1-N3C	1.930(6)	1.938(4)	1.945(8)	2.140(3)
Fe1-N4C	1.989(8)	1.986(4)	2.003(4)	2.179(3)
Fe1-N5	2.005(7)	2.002(3)	2.003(4)	2.069(3)
Fe1-N5C	2.011(8)	2.008(3)	2.017(4)	2.080(3)
N1-Fe1-N2	80.96(6)	80.60(15)	80.60(6)	74.84(10)
N1-Fe1-N3C	99.47(6)	98.04(15)	99.63(6)	103.44(9)
N1-Fe1-N4C	83.66(6)	83.35(14)	83.36(6)	81.89(10)
N1-Fe1-N5	166.43(6)	165.09(15)	165.88(7)	158.05(10)
N1-Fe1-N5C	93.42(6)	94.47(15)	93.49(6)	94.13(10)
N5-Fe1-N5C	91.80(9)	91.9(2)	92.24(9)	98.66(14)

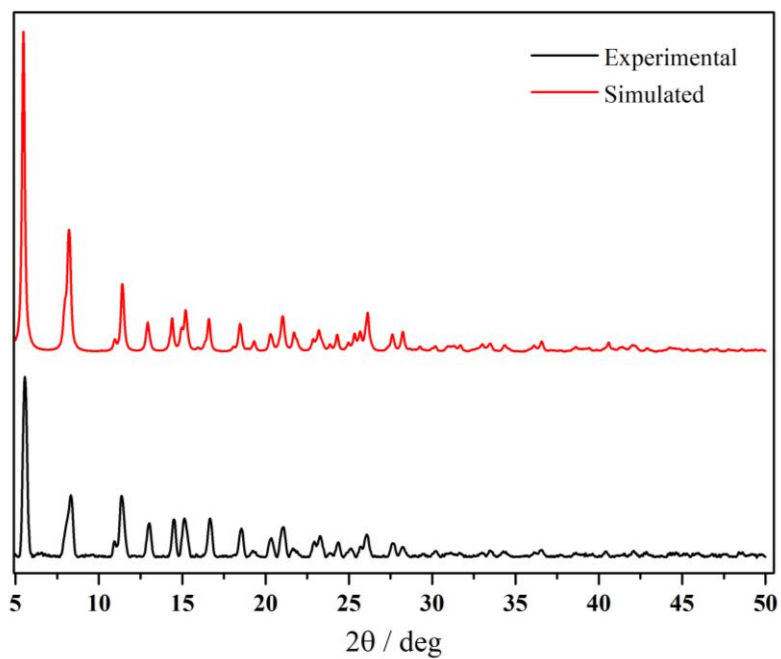


**Fig. S1.** The experimental and simulated PXR D patterns of **2** at 300 K.

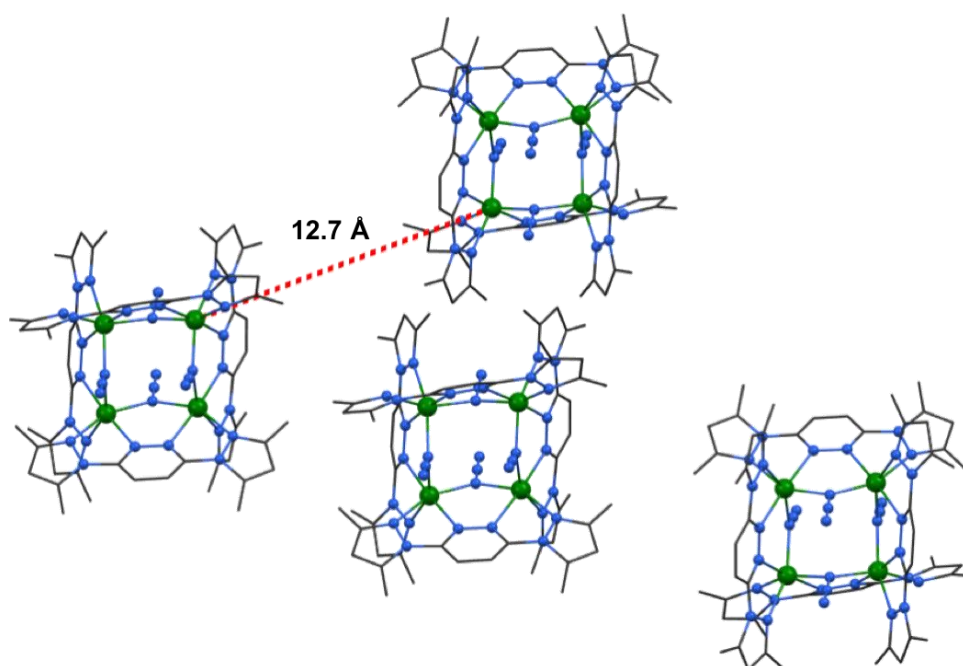


**Fig. S2.** The packing diagram of **1**. Hydrogen atoms, counter ions and lattice solvents are omitted for clarity.

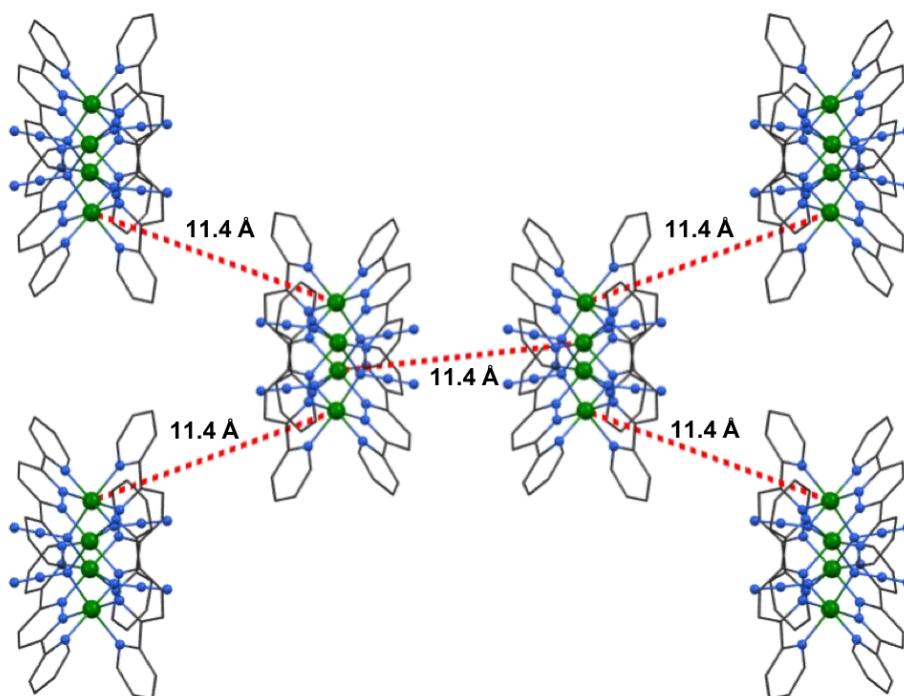


**Fig. S3.** The packing diagram of **2**. Hydrogen atoms, counter ions and lattice solvents are omitted for clarity.

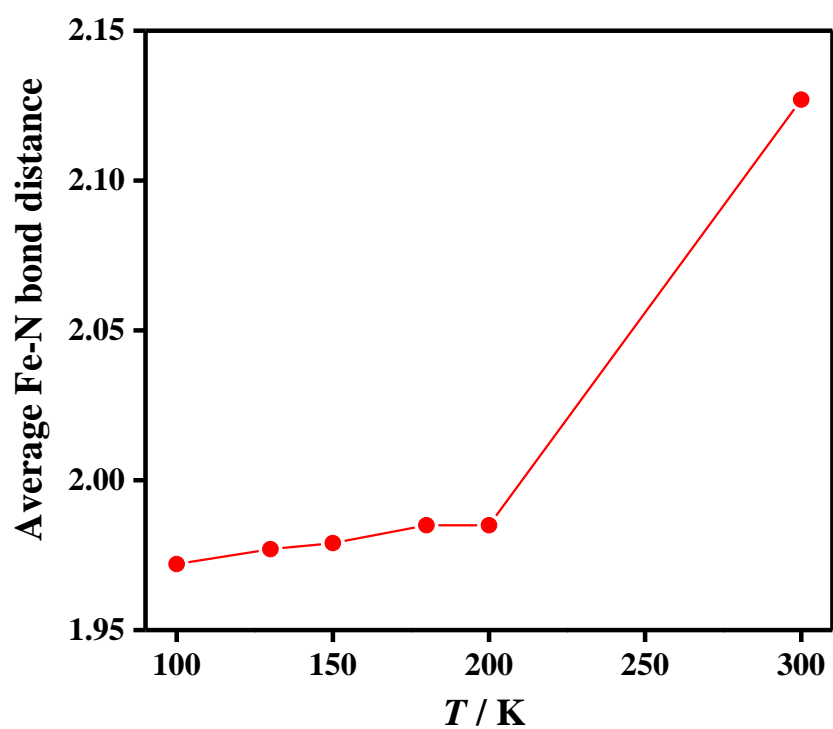


**Fig. S4.** Temperature dependence of average Fe-N bond distances for complex **2**. Solid lines are guided to the eye.

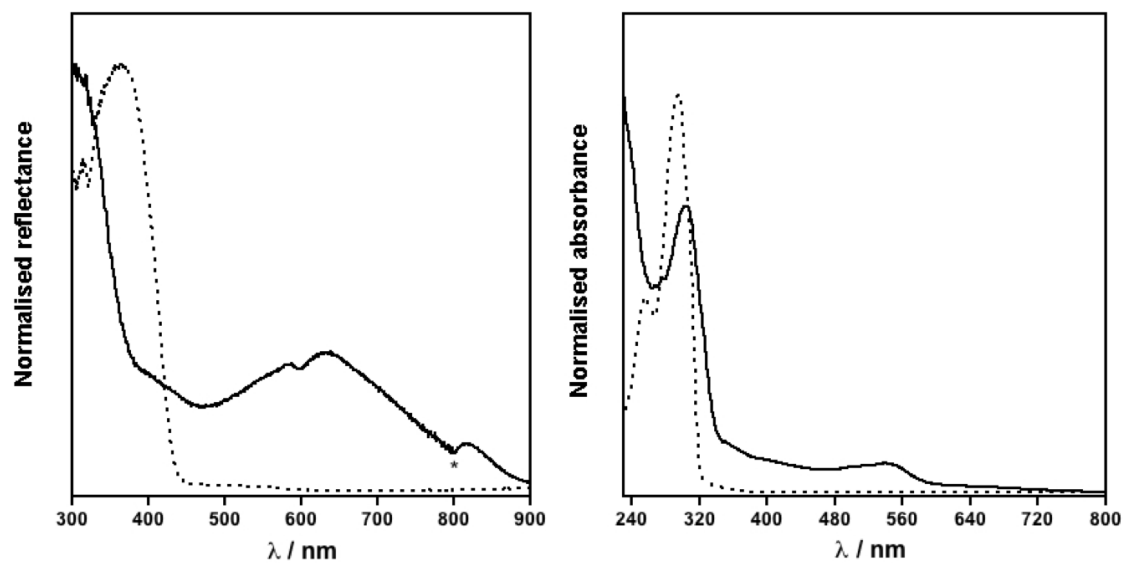


**Fig. S5.** Solid state (left) and acetonitrile solution (right) UV-vis spectra of **2** (solid line) and pydz ligand (dashed line) at room temperature (\* is an artifact due to lamp change at 800 nm).

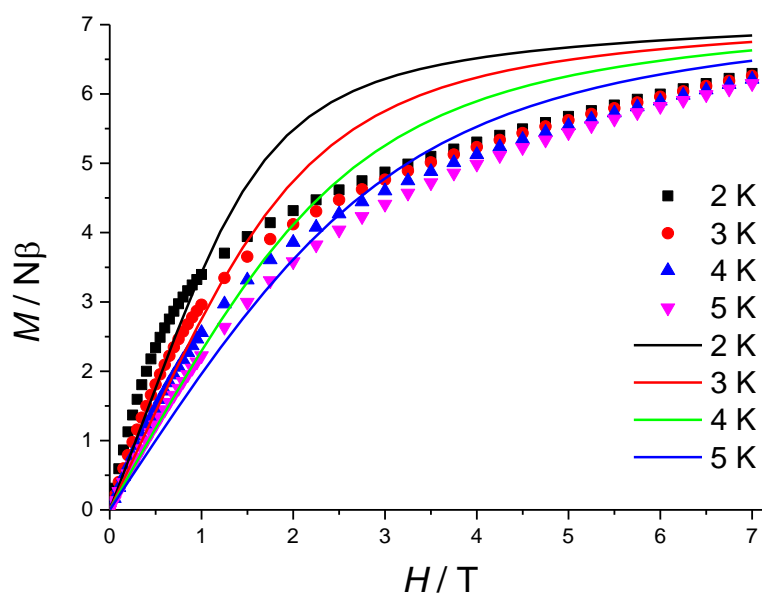


**Fig. S6.**  $M$  vs  $H$  data for **1** at 2-5 K. The solid lines represent the simulations using the spin Hamiltonian parameters from the  $\chi T$  fit.

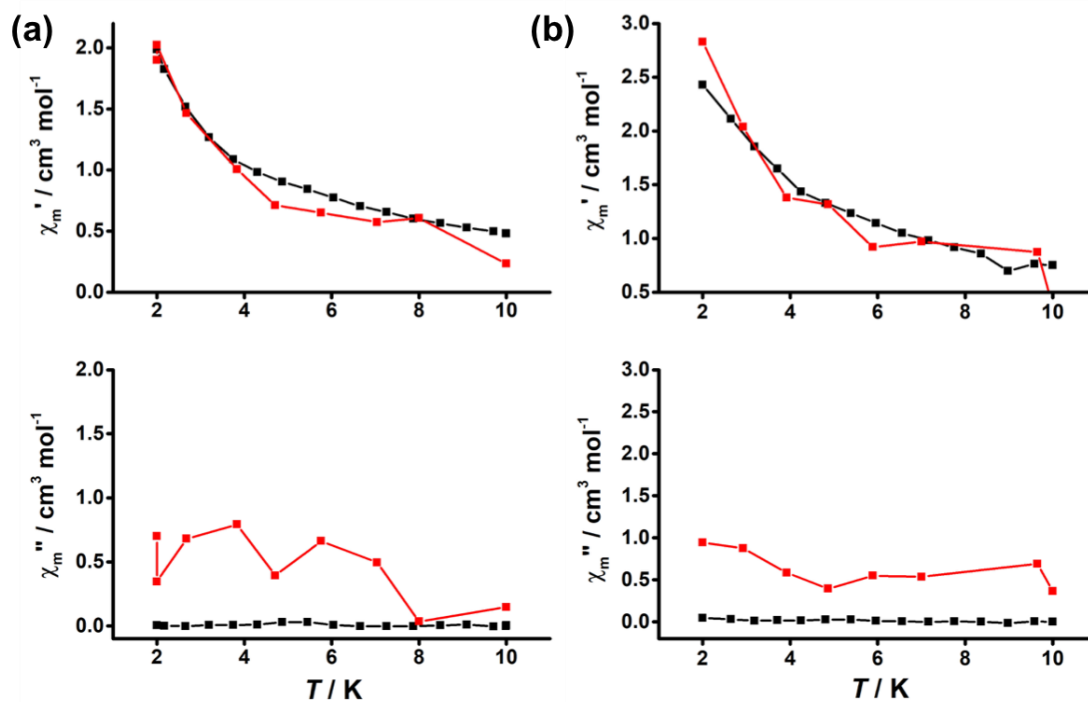


**Fig. S7.** AC magnetic susceptibility measurement of **1** under zero (a) and 1000 Oe (b) applied dc field.

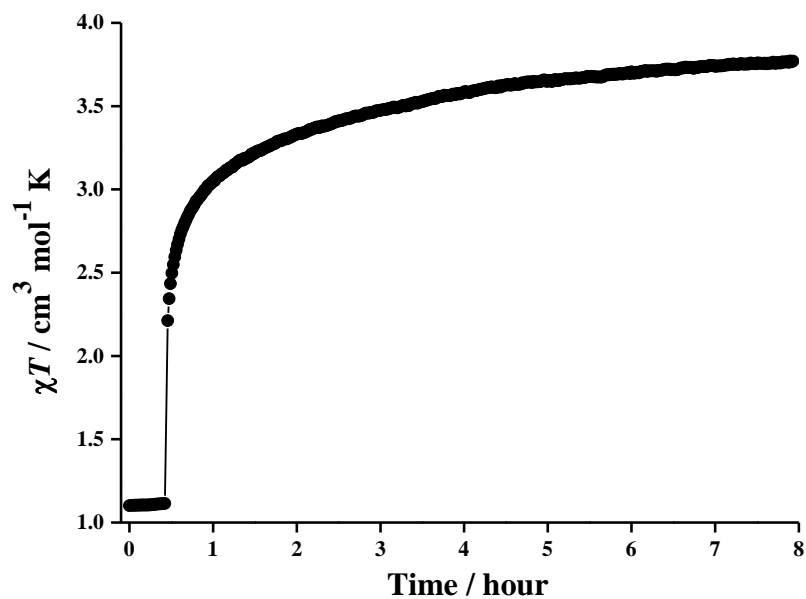


**Fig. S8.** Time evolution of the  $\chi T$  products of **2** at 10 kOe under light irradiation (808 nm, 10 mW) at 10 K.